Activation of 5-HT_7 receptors in the mouse dentate gyrus selectively enhances GABAergic inhibition of hilar mossy cells without affecting plasticity at the perforant path synapse

Marcin Siwiec [1*], Bartosz Bobula [1], Michał Kiełbiński [1], Nikola Multan [2], Grzegorz Hess [2], Krzysztof Tokarski [1]

[1] Department of Physiology, Maj Institute of Pharmacology, Polish Academy of Sciences, Smetna 12 Str., 31-343 Kraków, Poland

[2] Department of Neurophysiology and Chronobiology, Institute of Zoology and Biomedical Research, Faculty of Biology, Jagiellonian University, Gronostajowa 9 Str., 30-387 Kraków, Poland

* Corresponding author

E-mail address: siwiec@if-pan.krakow.pl

Running title: Effects of 5-HT_7 receptors in the dentate gyrus

Keywords

5-HT_7 receptors, hippocampus, dentate gyrus, LTP, mossy cells

Abstract

Background

The study examined the effects of 5-HT_7 receptor activation on GABAergic transmission within the dentate gyrus and plasticity at the glutamatergic perforant path input.

Methods

Immunofluorescence imaging was performed using transverse hippocampal slices from transgenic mice expressing GFP under the Htr7 promoter. This was followed by whole-cell patch clamp electrophysiological recordings of spontaneous inhibitory postsynaptic currents recorded from dentate granule cells and hilar mossy cells — two glutamatergic neuron types present in the dentate gyrus. Extracellular recordings of field excitatory postsynaptic potentials were then performed to assess whether 5-HT_7 receptor activation influenced theta burst stimulation-evoked plasticity of the perforant path synaptic input.

Results

It was found that parvalbumin and somatostatin interneurons in the dentate gyrus expressed GFP. Activation of 5-HT_7 receptors increased GABAergic transmission targeting mossy cells but not granule cells. However, there was no effect of 5-HT_7 receptor activation on perforant path plasticity either with intact or blocked $GABA_A$ receptor signaling.

Conclusion

The presence of 5-HT_7 receptors in a subset of parvalbumin and somatostatin interneurons in the mouse dentate gyrus could mean that they are involved in the inhibitory control of dentate gyrus activity, although the effect seems to be confined to mossy cells and did not translate to changes in perforant path plasticity. Further experiments are needed to fully elucidate the functional role of these receptors in the dentate gyrus.

Introduction

GABAergic transmission is a potent regulator of the plasticity of excitatory synapses [1,2]. Although the history of the research on long-term synaptic plasticity of perforant path synapses in the dentate gyrus (DG) goes back more than 50 years [3], its modulation by local DG interneurons remains incompletely understood. Perforant path synapses in the DG are capable of bidirectional plasticity (long-term potentiation, LTP, and long-term depression, LTD [4]). The primary neuronal type of the DG are small, glutamatergic granule cells forming the granular layer but in addition to several types of GABAergic interneurons [5], that are located mainly along the base of the granular layer and in the hilus, the DG contains also less numerous, large, glutamatergic mossy cells, residing in the hilus [6]. All these different neuronal types form within the DG a complex network of synaptic connections that functions as a gate for further information flow into the hippocampus proper [7,8].

An important factor involved in LTP modulation in the DG is the serotonergic innervation [9], acting via 5-HT_{1A} [10], 5-HT_{2C} [11] and 5-HT_4 [12] receptors. The 5-HT_7 receptor (5-HT_7R), the last member of the 5-HT receptor family to be identified [13–15], is abundant in the DG as well [16], however, its involvement in the induction of synaptic plasticity in the DG has not been investigated. Activation of 5-HT_7Rs enhances neuronal membrane excitability and/or spiking behavior in CA1 pyramidal neurons [17,18] so it is conceivable that 5-HT_7R activation might alter the conditions for the induction of synaptic plasticity in the DG.

Thus, to examine the pattern of 5-HT_7R expression in the DG, in the present study we used a transgenic mouse line expressing GFP under the Htr7 promoter. Following up on immunofluorescence results showing that GFP related to 5-HT_7R expression is present predominantly in DG inhibitory interneurons, further experiments focused on elucidating the functional consequences of 5-HT_7R activation on GABAergic control of the two excitatory cell types of the DG — granule cells and mossy cells. The final set of experiments aimed to characterize the potential effects of 5-HT_7R activation on the plasticity of the medial perforant path input to the DG.

Materials and Methods

Animals

Male wild-type and transgenic C57BL/6J mice were maintained on a 12/12 h light/dark schedule with standard food and tap water available *ad libitum*. The 5-HT_7-GFP strain used in the study — Tg(Htr7-EGFP)ST29Gsat/Mmucd — was generated as part of the GENSAT project [19].

Tissue preparation, immunofluorescent staining and imaging

Male 5-HT_7R-GFP mice were transcardially perfused with PBS followed by 4% paraformaldehyde (PFA) in 0.1M phosphate buffered saline (PBS). After a post-fixation period of 12h at 4 ℃, 50 μm-thick transverse brain sections were cut using a Leica VT-1200S vibrating blade microtome (Leica Microsystems). Free-floating sections were incubated in a blocking buffer containing 5% normal donkey serum (NDS, JacksonImmunoResearch) and 0.1% Triton X-100 (TX-100, Invitrogen) in PBS for 1h. Next they were incubated overnight at 4°C with the following primary antibodies diluted in the blocking buffer: 1:1000 chicken anti-GFP (Aves Labs GFP-1020), 1:200 mouse anti-somatostatin (GeneTex SOM-018), 1:1000 rabbit anti-parvalbumin (PV27, SWANT). Another combination of primary antibodies used was 1:1000 chicken anti-GFP with 1:1000 mouse anti-calretinin (6B3, SWANT) and 1:1000 rabbit anti pro-CCK (107-115aa, Frontier Institute). After extensive 3 × 10 min washing in PBS, the slices were further incubated in a mixture of the following secondary antibodies for 1h at room temperature: goat anti-chicken Alexa Fluor Plus 488, goat anti-mouse Alexa Fluor Plus 555, goat anti-rabbit Alexa Fluor Plus 647 (all from Invitrogen). Subsequently, sections were washed in PBS, counterstained with DAPI, washed again, mounted, and coverslipped with Prolong Glass antifade medium (Invitrogen). Optical z-stacks were then captured with a 20x/0.8 air objective (Plan-Apochromat 20x/0.8 M27) and Axiocam 506 camera on a Zeiss Axio Imager Z2 fluorescence microscope equipped with the Apotome 2 optical sectioning module (Carl Zeiss, Germany).

The proportion of GFP-expressing parvalbumin (PV^+) and somatostatin (SOM^+) interneurons was assessed using microphotographs from 3 mice (5-6 sections per animal). Images were automatically

processed with FIJI/ImageJ scripts [20]. The workflow consisted of per-channel background subtraction (rolling ball method), followed by automated local thresholding. Bernsen, IsoData and moments segmentation algorithms were used for PV, SOM and GFP signals, respectively, based on empirical testing in example images. Thresholded images were size-filtered to retain objects corresponding to intact and fully stained neuronal somata. Colocalization was assessed separately in each optical slice using the pixel value product method, followed by manual verification and, finally, z-projection and cell counting.

Brain slice preparation for electrophysiological experiments

Mice were decapitated under isoflurane anesthesia (Aerrane, Baxter). Their brains were quickly removed and placed in cold neuroprotective artificial cerebrospinal fluid (NMDG-HEPES ACSF) containing (in mM): 92 NMDG, 2.5 KCl, 0.5 $CaCl_2$, 10 $MgSO_4$, 1.2 NaH_2PO_4, 30 $NaHCO_3$ 20 HEPES, 25 glucose, 5 sodium ascorbate, 2 thiourea, 3 sodium pyruvate, pH titrated to 7.3 with HCl. Transverse 350 µm slices containing the ventral/intermediate dentate gyrus were cut on a vibrating microtome (Leica VT1200S, Leica Microsystems) and incubated at 35°C for 25 min in NMDG-HEPES aCSF while gradually introducing NaCl [21]. Afterwards, slices were transferred to the HEPES holding ACSF containing (in mM): 92 NaCl, 2.5 KCl, 1.2 NaH_2PO_4, 30 $NaHCO_3$, 20 HEPES, 25 glucose, 5 sodium ascorbate, 2 thiourea, 3 sodium pyruvate, 2 $MgSO_4$, 2 $CaCl_2$, pH titrated to 7.3 with NaOH, and held at room temperature for at least one hour before recording. ACSF was continuously bubbled with 95% O_2 and 5% CO_2. Solution osmolality was 300-310 mOsm. All compounds for ASCF solutions were purchased from Sigma-Aldrich.

Whole-cell patch clamp recordings of spontaneous inhibitory postsynaptic currents

Slices were placed in the recording chamber and superfused at 4-5 ml/min with warm (32 ± 0.5°C) recording ACSF composed of (in mM): 132 NaCl, 2 KCl, 2.5 $CaCl_2$, 1.3 $MgSO_4$, 1.2 NaH_2PO_4, 24 $NaHCO_3$ and 10 glucose, continuously bubbled with a mixture of 95% O_2 and 5% CO_2. Neurons were visualized on a Nikon Eclipse Fn1 upright microscope (Nikon Europe B.V.) equipped with 900 nm IR

DIC optics, a 40×0.8 NA water immersion objective and sCMOS camera (CellCam Kikker, Cairn Research), along with a computer-controlled piezo xy stage and micromanipulators (Sensapex). Patch pipettes were pulled from 1.5 mm OD/0.86 mm ID borosilicate glass capillaries (Sutter Instruments) using a P87 puller (Sutter Instruments). Spontaneous inhibitory postsynaptic currents (sIPSCs) were recorded from dentate granule cells as well as hilar mossy cells in whole-cell voltage clamp mode using a Multiclamp 700B amplifier (Molecular Devices). Signals were filtered at 2 kHz and digitized at 20 kHz with a National Instruments PCIe-6353 data acquisition card controlled by the open-source ACQ4 software package [22]. Biocytin (0.3%, HelloBio) was included in the recording pipette solution for later verification of cell morphology. A high-chloride recording pipette solution was used for recording sIPSCs and contained (in mM): 130 KCl, 5 NaCl, 0.3 $CaCl_2$, 2 $MgCl_2$, 10 HEPES, 10 phosphocreatine-Na_2, 5 Na_2-ATP, 0.4 Na-GTP and 0.3 EGTA. Osmolarity and pH were adjusted to 290 mOsm and 7.2 respectively. Recording pipettes had open tip resistances of approximately 4-6 MΩ when filled with this solution. The AMPA/kainate receptor blocker NBQX (10 μM, HelloBio) was included in the recording ACSF to isolate GABAergic synaptic activity. A holding potential of −76 mV was used to reliably record sIPSCs with few/no action potential currents present. Cell identification was based on anatomical location (mossy cells — dentate gyrus hilar region; granule cells — the outer third part of the granule cell layer in the supra-pyramidal blade of the ventral/intermediate dentate gyrus), electrophysiological properties and cell morphology. Typical dentate granule cells had a small ovoid cell body and were characterized by a relatively hyperpolarized resting membrane potential recorded right after break-in (typically ~ −80 mV). They also displayed a typical membrane resistance of 200-300 MΩ and low intrinsic excitability [23]. Hilar mossy cells, on the other hand, typically had large, triangular or trapezoidal cell bodies. Upon break-in, they were characterized by a large cell capacitance, membrane resistance of 150-300 MΩ, relatively higher excitability and high magnitude, frequent spontaneous synaptic activity [24]. After recording cells were further confirmed to belong to these two neuronal populations on the basis of dendritic morphology revealed by biocytin labeling.

Morphological verification of recorded cells

Slices were fixed in 4% PFA in PBS for 1 h. After several washing steps, they were incubated in PBS containing 0.1% TX-100 and Alexa Fluor 647-conjugated streptavidin (1:500, Invitrogen) for 2 h at RT on an orbital shaker. After washing in PBS and counterstaining with DAPI (Invitrogen) slices were mounted on glass slides and coverslipped using the Vectashield mounting medium (Vector Laboratories). Verification of individual neuron morphology was performed after acquiring z-stacks taken with a 20×0.8 NA air apochromatic objective on a Zeiss Axio Imager Z2 fluorescence microscope using the Apotome 2 module (Carl Zeiss).

Extracellular recordings of medial perforant path-dentate gyrus plasticity

Extracellular recordings were performed using the same ACSF and hardware as the patch clamp recordings. The WinLTP software package was used for recording of plasticity experiments [25]. In a subset of recordings 100 μM picrotoxin (HelloBio) was added to the ACSF to block inhibitory transmission via $GABA_A$ receptors. Field extracellular excitatory postsynaptic potentials (fEPSPs) were elicited using a concentric bipolar stimulation electrode (FHC) placed in the middle of the dentate gyrus molecular layer of the suprapyramidal blade, corresponding to the medial perforant path. The recording electrode (3-5 MΩ patch clamp recording pipette filled with recording ACSF) was placed approximately 200-400 μm away from the stimulating electrode (Fig. 4). Monosynaptic fEPSPs were elicited every 20 s with 200 μs current pulses using a constant-current stimulus isolation unit (WPI). After a 10-15 min stabilization period, the stimulation intensity was adjusted to evoke fEPSPs with a rising slope approximately 50% of the maximum value (typically 20-30 μA). A theta-burst stimulation (TBS) protocol was used to induce plasticity after recording a 20 min baseline period. TBS consisted of a series of 5 high-frequency 100 Hz 200 μs pulses repeated five times every 200 ms. This was repeated 5 times every 10 s. The TBS protocol was chosen for a physiologically plausible LTP induction mechanism [26]. After TBS the recordings continued for 1 h with baseline stimulation intensity.

Pharmacological activation of 5-HT$_7$ receptors

Drugs were bath-applied in final concentrations for both patch clamp and extracellular recordings. The selective 5-HT$_7$R agonist LP-211 (Sigma-Aldrich) was dissolved in dimethyl sulfoxide (DMSO, HelloBio) and diluted in ACSF to a final concentration of 1 μM (LP-211) and 0.1% v/v (DMSO). LP-211 has been extensively used in functional studies of 5-HT$_7$Rs [27–31]. Control and/or baseline recordings were performed in 0.1% DMSO alone. The highly selective 5-HT$_7$R antagonist SB 269970 (2 μM, HelloBio) was used in a subset of recordings to confirm the selectivity and specificity of any LP-211-evoked effects. The slice was perfused with the antagonist for at least 15 min before commencing recordings.

In patch clamp experiments the effect of LP-211 on GABAergic transmission was evaluated relative to baseline levels in each cell. After obtaining the whole-cell configuration and verifying the electrophysiological phenotype of the recorded cell in current clamp mode using a series of hyper- and depolarizing current pulses, the recording was switched to voltage clamp at −76 mV and after several minutes of stabilization a 4 min baseline period of sIPSC activity was recorded in ACSF containing 10 μM NBQX and 0.1% DMSO. Next, the perfusion line was switched to ACSF containing 10 μM NBQX with 1 μM LP-211 in 0.1% DMSO and the slice was perfused for 12 min to allow the compound to activate the receptors and equilibrate before recording another 4 min period. Access resistance had to stay below 20 MΩ and not change by more than 20%, otherwise the recording was discarded. For extracellular experiments, 1 μM LP-211 was added to the ACSF and allowed to perfuse the slice approximately 1 h before the planned induction of plasticity, i.e. 30 min before starting the recording. In control recordings 0.1% DMSO alone was used within the same time frame.

Electrophysiology data analysis and statistics

For patch clamp experiments and sIPSC detection, the 4 min “baseline” and “LP-211” segments were analyzed to detect sIPSCs using a deconvolution algorithm [32] implemented in the Eventer software package [33]. Extracellular recordings were analyzed using WinLTP software [25], where three consecutive fEPSP traces (stimulation every 20 s) were averaged to obtain one low-noise reading of

fEPSP slope for every minute of the recording. The maximum slope was calculated from the rising slope of the fEPSP in a sliding 1.5 ms time window. The data were then normalized to the mean slope of the 20 min baseline period for each recording separately. The final values for plasticity magnitude were thus expressed as percentages of the mean baseline slope level. Statistical data analysis and graphing of the results was performed using the R programming language and RStudio IDE [34,35]. R packages used were the tidyverse collection [36] and patchwork [37]. Statistics on sIPSC frequency and amplitude before and after LP-211 administration were performed using a two-tailed paired samples t-test. Due to the bidirectionality of plasticity results and resulting lack of normality, extracellular recordings were analyzed by comparing whole distributions of plasticity magnitudes between the control and experimental groups using the nonparametric two-sample Kolmogorov-Smirnov test. The resulting distributions were plotted as cumulative probability histograms using the ecdf() R function. For all statistical procedures, inference was two-tailed and performed with the arbitrary significance threshold set at $p < 0.05$. Extracellular summary fEPSP data were plotted as mean ± SEM.

Results

Htr7 promoter-dependent GFP is expressed in PV and SOM interneurons in the mouse dentate gyrus

The observed GFP immunostaining pattern in 5-HT_7R-GFP mice consisted of sparse, but distinct, labeling of neuronal cell bodies, which, in transverse sections of the dentate gyrus, were primarily located in the hilus, with only single immunopositive cells present in the granule and molecular layers. These GFP^+ cells were presumptive inhibitory interneurons predominantly co-expressing SOM or PV (Fig. 1), but typically not calretinin or pro-cholecystokinin. For the latter two markers, only a handful of cells with weak fluorescent signal corresponding to putative GFP expression were found (not shown). Quantification of PV and SOM cell bodies revealed GFP co-expression was widespread in these populations, as double-immunopositive cells constituted 59% (223/379) of all PV^+ and 70% (271/382) of all SOM^+ neurons.

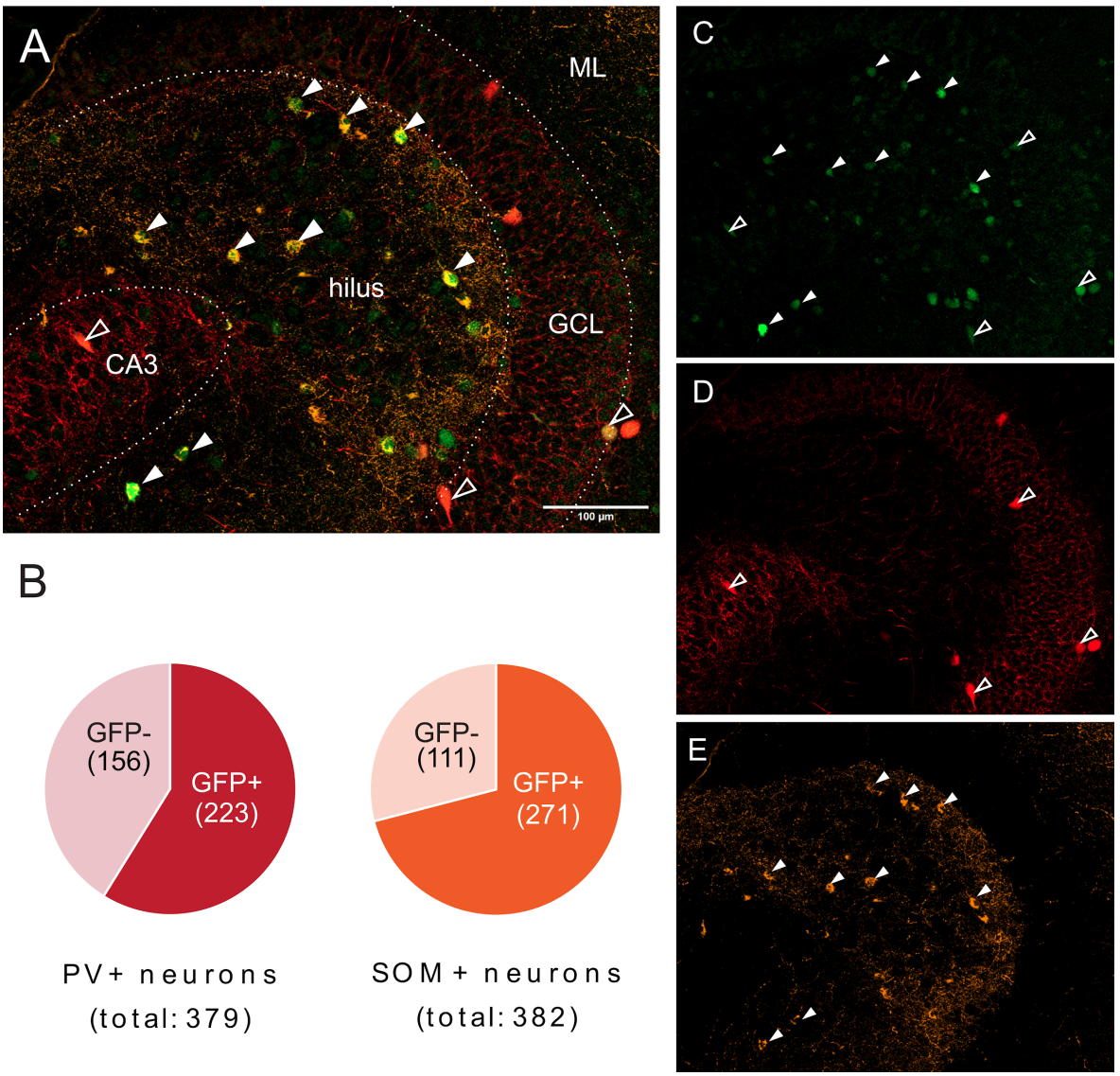

Figure 1. Representative composite frame image (A) and corresponding single channel images of a mouse dentate gyrus section stained for GFP (green; B), SOM (yellow; C) and PV (red; D). Cell bodies immunopositive for SOM–GFP and PV–GFP indicated with solid arrowheads and contour arrowheads, respectively.

Activation of 5-HT$_7$ receptors does not equally affect inhibitory transmission targeting granule cells and mossy cells

Since GFP related to 5-HT$_7$R was expressed predominantly in inhibitory interneurons, further experiments focused on functional consequences of 5-HT$_7$R activation on the GABAergic input to the two DG excitatory cell types. Whole-cell recordings of sIPSCs in granule cells revealed that activation of 5-HT$_7$Rs by LP-211 did not influence the inhibitory transmission targeting this cell type (Fig. 2). LP-211 did not affect sIPSC frequency (10.9 ± 1.14 Hz vs. 11.7 ± 1.51 Hz, $t(31) = -0.849$, p =

0.402, paired samples t-test) or amplitude (22.9 ± 1.02 pA vs. 24.3 ± 1.07 pA, t(31) = -1.83, p = 0.0776, paired samples t-test).

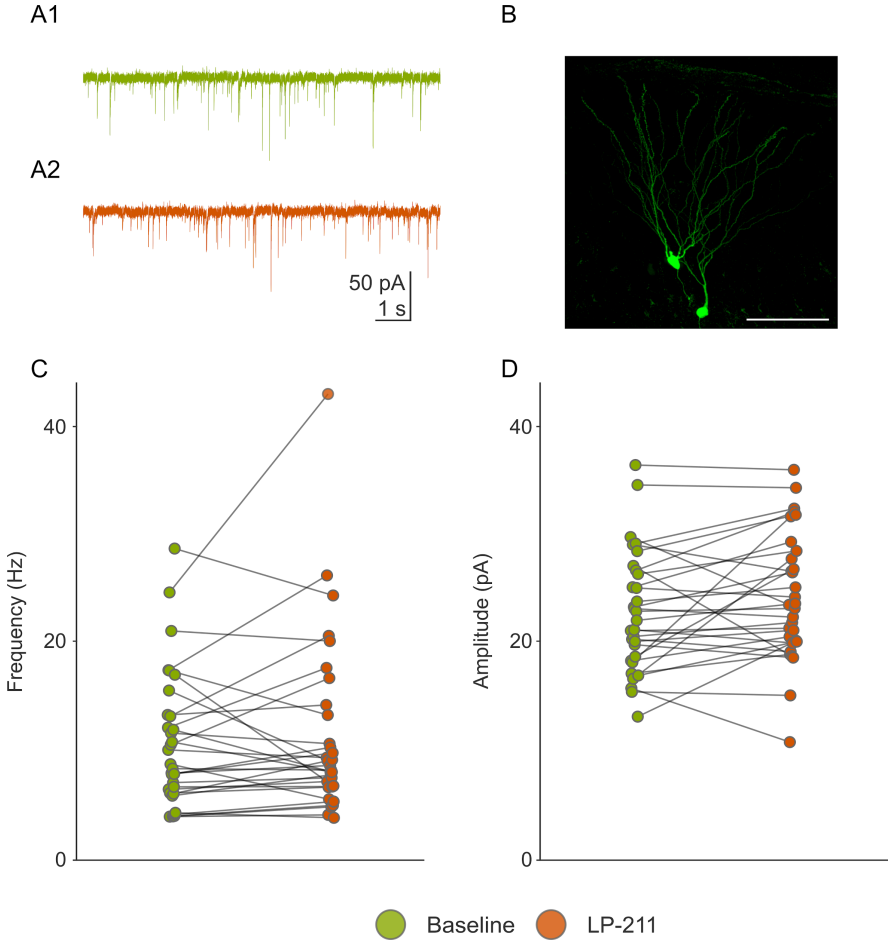

Figure 2. Effects of LP-211 on GABAergic transmission targeting dentate gyrus granule cells. (A1, A2) Raw sIPSC traces before and after LP-211 administration respectively. (B) Maximum projection image of representative biocytin-filled granule cells. Calibration bar = 100 µm. Application of 1 µM LP-211 did not affect sIPSC frequency (C — p = 0.402, paired samples t test) or amplitude (D — p = 0.0776, paired samples t test).

In contrast, recordings from mossy cells revealed that LP-211 increased the frequency of sIPSCs (18.2 ± 2.15 Hz vs. 23.8 ± 3.73 Hz, t(21) = -2.27, p = 0.0347, paired samples t-test) without affecting the amplitude (31.6 ± 4.01 pA vs. 31.5 ± 3.10 pA, t(21) = 0.0301, p = 0.976, paired samples t-test; Fig. 3). Preincubation of slices with the selective 5-HT_7R antagonist SB 269970 prevented the increase in sIPSC frequency (18.4 ± 3.03 Hz vs. 17.5 ± 2.81 Hz, t(6) = 0.984, p = 0.37, paired samples t-test; Fig. 3) and preserved the lack of change in sIPSC amplitude (27.2 ± 5.96 pA vs. 25.4 ± 5.91 pA, t(6) = 1.28, p = 0.258, paired samples t-test).

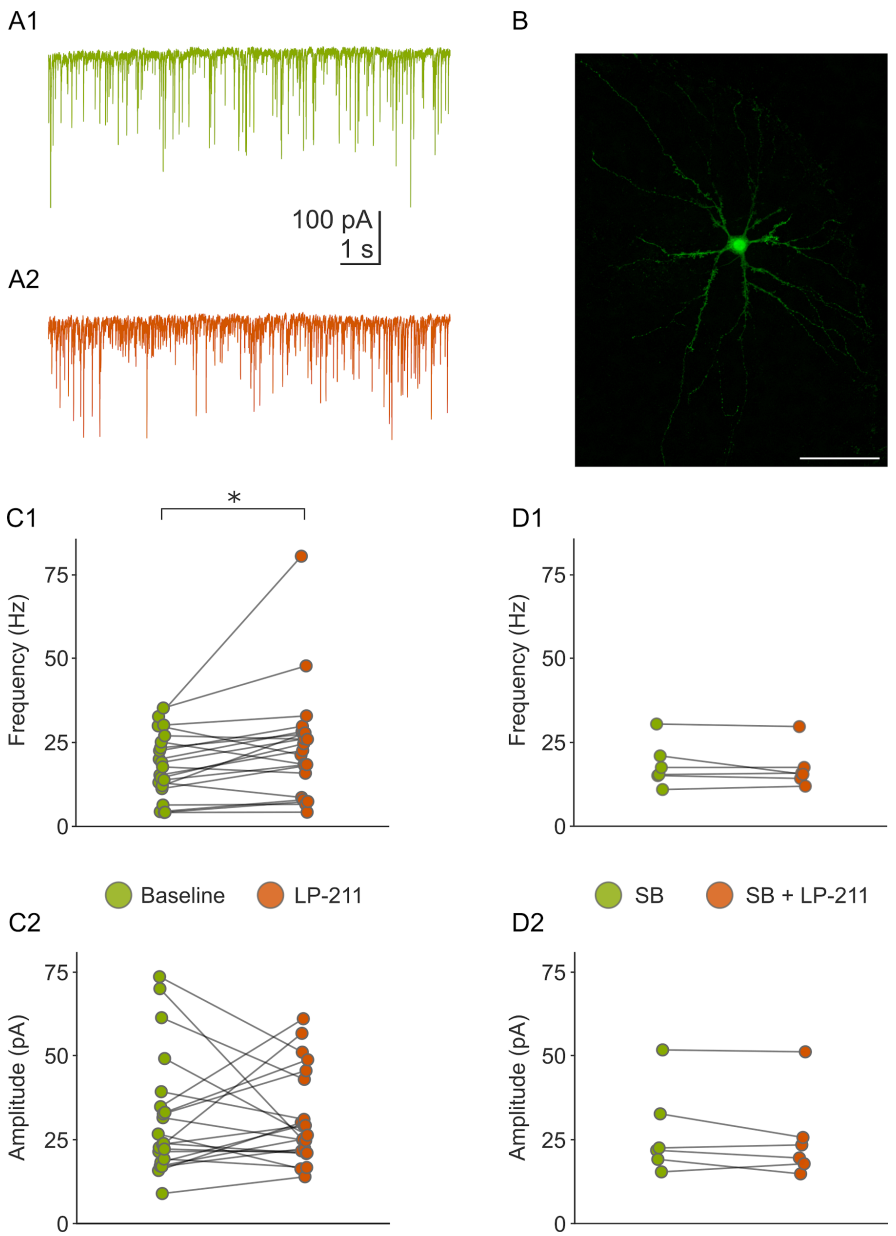

Figure 3. Effects of LP-211 on GABAergic transmission targeting hilar mossy cells. (A1, A2) Raw sIPSC traces before and after LP-211 administration respectively. (B) Maximum projection image of a representative biocytin-filled mossy cell. Calibration bar = 100 µm. Application of 1 µM LP-211 increased sIPSC frequency (C1 — $p = 0.0347$, paired samples t test) without affecting the amplitude (C2 — $p = 0.976$, paired samples t test). Preincubation of slices with the selective 5-HT7R antagonist SB 269970 prevented the increase in sIPSC frequency (D1 — $p = 0.37$, paired samples t test) and preserved the lack of change in sIPSC amplitude (D2 — $p = 0.258$, paired samples t test).

Activation of 5-HT$_7$ receptors does not affect the theta-burst-evoked plasticity of the medial perforant path-granule cell synapse

To characterize potential effects of 5-HT$_7$R activation on the plasticity of the medial perforant path input to the DG, fEPSPs evoked by stimulation of the medial perforant path were recorded. In conditions with intact GABAergic signaling TBS failed to induce LTP with the majority of recordings resulting in no LTP or even LTD and the mean plasticity magnitude of 85.3 ± 8.32% relative to baseline (i.e. 100%; Fig. 4 A1-A2). Activation of 5-HT$_7$Rs by preincubating slices with ACSF containing 1 μM LP-211 did not change this distribution of plasticity magnitudes ($D_{17,17}$ = 0.23529, p = 0.75061, exact two-sample Kolmogorov-Smirnov test), with the mean plasticity magnitude in the LP-211 group of 87.5 ± 5.13%. The exact same plasticity induction protocol resulted in a robust LTP when 100 μM picrotoxin (PTX) was added to the ACSF to block fast GABAergic inhibition (Fig. 4 B1-B2), with the mean plasticity magnitude of 153 ± 24%. This time the distribution of plasticity magnitudes strongly favored LTP over LTD, however, when LP-211 was included in the recording ACSF the distribution of plasticity magnitudes remained unchanged ($D_{19,13}$ = 0.27126, p = 0.51867, exact two-sample Kolmogorov-Smirnov test), with the mean plasticity magnitude of 166 ± 28% (Fig. 4 C1-C2).

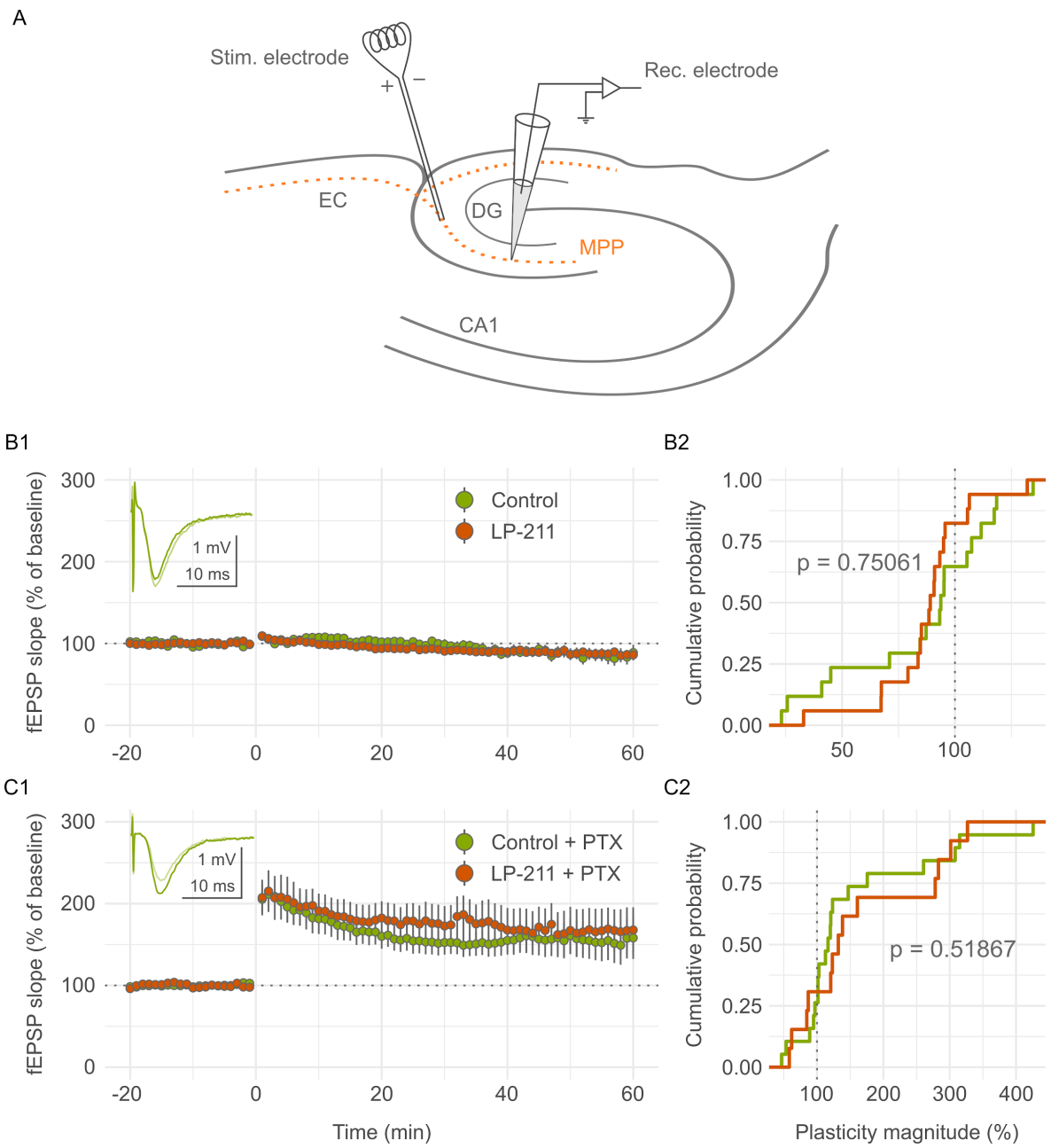

Figure 4. Effects of LP-211 on the magnitude of medial perforant path-dentate gyrus plasticity. (A) Anatomical diagram showing the placement of recording and stimulation electrodes. Abbreviations: EC — entorhinal cortex; CA1 — cornu Ammonis 1; DG — dentate gyrus; MPP — medial perforant path. (B1) Effects of LP-211 preincubation on fEPSP slope (%) before and after TBS. Inset: raw fEPSP traces of a representative control recording before (lighter green) and after (darker green) TBS. (B2) Cumulative probability histograms showing that preincubation of slices with LP-211 did not affect the distribution of plasticity magnitudes ($p = 0.75061$, exact two-sample Kolmogorov-Smirnov test). (C1) Effects of LP-211 preincubation on fEPSP slope (%) before and after TBS with 100 μM picrotoxin (PTX) present in the ACSF to block $GABA_A$ receptors. Inset: raw fEPSP traces of a representative control recording before (lighter green) and after (darker green) TBS. (C2) Cumulative probability histograms showing that preincubation of slices with LP-211 with PTX present in the ACSF did not affect the distribution of plasticity magnitudes ($p = 0.51867$, exact two-sample Kolmogorov-Smirnov test).

Discussion

The results of this study indicate that in the dentate gyrus 5-HT_7Rs are expressed predominantly on inhibitory interneurons of the hilar region. However, activation of these receptors selectively enhances inhibitory synaptic input to mossy cells but not granule cells.

It has been shown that mossy cells function as local circuit integrators and exert modulatory influence on dentate granule cells as well as the CA3 through back-projecting pathways [38,39]. They receive considerable excitatory synaptic input from granule cells' massive specialized synaptic boutons (mossy terminals) apposed to thorny excrescences present on their cell bodies and proximal dendrites giving them their "mossy" appearance [40]. In turn, mossy cells are monosynaptically coupled to granule cells both ipsi- and contralaterally. However, this connection is only weakly excitatory, prone to synaptic failures and strongly masked by GABAergic inhibition. Therefore it is believed that the primary effect of mossy cell activation on granule cells is in fact non-direct and inhibitory, via the excitation of local GABAergic interneurons [41], with some studies suggesting that this interaction can become reversed in pathological states of hippocampal circuit activity such as those resulting from acute trauma and epileptogenesis [42,43]. Furthermore, direct excitatory connections have also been discovered between individual mossy cells, which could in theory further consolidate their influence on granule cell activity [44].

Given the considerable glutamatergic drive via mossy terminals, the activity of mossy cells has to be tightly controlled by various subtypes of dentate and hilar interneurons [45–47]. We have not identified the interneurons that form the inhibitory input to mossy cells, however, it is likely that this input is at least partially provided by hilar somatostatin-positive cells [40,48]. Activation of 5-HT_7Rs by LP-211 and the subsequent increase in GABAergic transmission recorded from mossy cells is most probably a direct result of increased spiking activity of these interneurons, as 5-HT_7Rs are known enhancers of neuronal excitability [17,18,49,50]. However, it is important to note that somatostatin interneurons also regulate granule cell activity and the question remains as to why we did not record increased GABAergic transmission in those cells. One possible explanation is that the majority of

somatostatin interneurons targeting dentate granule cells are the so-called hilar perforant path-associated (HIPP) interneurons, which are characterized by weak, slow and unreliable inhibition of granule cell distal dendrites in the outer molecular layer, in contrast to strong, fast and reliable perisomatic inhibition coming from parvalbumin basket cells [47]. Any increase in somatostatin interneuron spiking activity would have to be strong enough to overcome the weak synaptic coupling in order to be reliably detected by somatic granule cell recordings. In the case of mossy cells, however, their thick proximal dendrites [51] are presumably characterized by lower axial resistances compared to thin granule cell dendrites and thus are more conductive to postsynaptic currents. Moreover, recently, a second subpopulation of dentate somatostatin interneurons was characterized in addition to HIPP cells — the so-called hilar interneurons (HILs), whose axon collaterals extensively innervate the dentate hilar region where mossy cell somata are located [48]. Further research is needed to characterize the degree of connectivity between these two neuron types, however activation of 5-HT_7Rs on HIL cells could in theory explain the increased sIPSC frequency recorded in mossy cells.

There are limited sources in the literature concerning if and how parvalbumin-positive interneurons innervate hilar mossy cells. However, the majority of parvalbumin interneurons in the dentate gyrus are basket cells characterized by large triangular cell bodies in the subgranular layer and extensive, basket-like branching of axon collaterals around granule cell somata, with few axons present in the hilus [47]. As for the rest of the parvalbumin interneuron cell population, not much is known about their postsynaptic targets and these may in fact include mossy cells. However, it is important to note that in general, hippocampal parvalbumin interneurons have different electrophysiological characteristics compared to their somatostatin counterparts. Although they are usually fast-spiking neurons, they have a lower input resistance and a more hyperpolarized resting membrane potential [47], and are often quiescent in standard *ex vivo* slice recording conditions. Therefore activation of 5-HT_7Rs located on these cells might not provide a depolarization strong enough for spontaneous spiking to occur, at least not in standard, baseline conditions such as those employed in this *ex vivo* study. Given that we demonstrate robust 5-HT_7R-GFP labeling of dentate parvalbumin interneurons, future experiments would need to study its functional implication *in vivo* or during *in vivo*-like

activity patterns evoked pharmacologically or electrically, where different classes of GABAergic interneurons would be driven to spiking.

One such attempt was made in this study, where we performed extracellular recordings measuring the synaptic plasticity of the medial perforant path input to the dentate gyrus. A theta-burst stimulation protocol was chosen (Fig. 4), as it reliably evokes hippocampal LTP and is physiological in nature (theta frequency hippocampal oscillations) in contrast to the more commonly used high frequency stimulation paradigm [26,52,53]. The dentate gyrus perforant path input is under strong GABAergic control and without blocking $GABA_A$ receptors it is highly resistant to LTP and even prone to LTD, as shown in our experiments. However, it was in principle possible for the 5-HT_7R-evoked increase in GABAergic inhibition of mossy cells to shift the distribution of plasticity magnitudes. Somewhat surprisingly, preincubation of slices in ACSF containing LP-211 did not affect the distribution of plasticity magnitudes either with intact or blocked fast GABAergic transmission. One possible explanation for this lack of effect is that, as we demonstrated, only GABAergic transmission to mossy cells was affected by 5-HT_7R activation, with no changes in sIPSCs recorded from granule cells. Mossy cells are potent regulators of granule cell activity, however they usually form translaminar or even contralateral connections, which are inevitably severed in transverse slice preparations typically employed to study hippocampal plasticity [40]. Another possibility is that 5-HT_7R-expressing interneurons are simply not recruited strongly enough by the TBS protocol for the 5-HT_7R activation to be able to reliably influence plasticity. Especially since GABAergic transmission targeting granule cells — whose dendrites are the source of fEPSP signal in extracellular recordings of perforant path plasticity — did not change following 5-HT_7R activation.

In spite of decades of research, serotonergic control of hippocampal activity remains an important research topic, perhaps because of the multitude of serotonin receptors and their associated molecular pathways, not to mention their role in various brain circuit pathologies. To date, many serotonin receptor subtypes have been identified in the dentate gyrus including, but not limited to 5-HT_{1A}, 5-HT_{1B}, 5-HT_{1D}, 5-HT_{2A}, 5-HT_{2C}, 5-HT_3, 5-HT_4, 5-HT_{5A}, 5-HT_6 and 5-HT_7 [12,54–62]. This study, while providing preliminary insights into the function of 5-HT_7Rs in the dentate gyrus, in fact resulted

in more questions than answers, for example about the functional consequences of 5-HT_7R activation on dentate gyrus circuit activity and synaptic plasticity *in vivo*. Or the precise somatostatin and parvalbumin interneuron subtypes which express these receptors. Successfully answering these and other questions in future studies could lead the scientific community to a better understanding of the role of the serotonin system in health and disease.

Funding

This work was supported by the National Science Centre, Poland, grant 2016/23/N/NZ4/03224.

Conflict of interest

The authors have no relevant financial or non-financial interests to disclose.

Author Contributions

MS designed the study, performed immunofluorescent staining, patch clamp and extracellular recordings, analyzed the data, prepared Figs. 2, 3, 4, wrote and revised the manuscript. BB performed extracellular recordings and analyzed the data. MK analyzed immunofluorescence images and prepared Fig. 1. NM performed extracellular recordings. GH helped conceptualize the study, wrote and revised the manuscript, provided guidance and supervision. KT helped conceptualize the study, revised the manuscript, provided guidance and supervision. All authors revised and approved the final manuscript.

References

[1] Chapman CA, Nuwer JL, Jacob TC. The Yin and Yang of GABAergic and Glutamatergic Synaptic Plasticity: Opposites in Balance by Crosstalking Mechanisms. Front Synaptic Neurosci 2022;14:911020. https://doi.org/10.3389/fnsyn.2022.911020.

[2] Khodaie B, Edelmann E, Leßmann V. Distinct GABAergic modulation of timing-dependent LTP in CA1 pyramidal neurons along the longitudinal axis of the mouse hippocampus. iScience 2024;27. https://doi.org/10.1016/j.isci.2024.109320.

[3] Caya-Bissonnette L, Béïque J-C. Half a century legacy of long-term potentiation. Current Biology 2024;34:R640–62. https://doi.org/10.1016/j.cub.2024.05.008.

[4] Koranda JL, Masino SA, Blaise JH. Bidirectional synaptic plasticity in the dentate gyrus of the awake freely behaving mouse. Journal of Neuroscience Methods 2008;167:160–6. https://doi.org/10.1016/j.jneumeth.2007.08.001.

[5] Houser CR. Interneurons of the dentate gyrus: an overview of cell types, terminal fields and neurochemical identity. Progress in Brain Research, vol. 163, Elsevier; 2007, p. 217–811. https://doi.org/10.1016/S0079-6123(07)63013-1.

[6] Kecskés A, Czéh B, Kecskés M. Mossy cells of the dentate gyrus: Drivers or inhibitors of epileptic seizures? Biochimica et Biophysica Acta (BBA) - Molecular Cell Research 2022;1869:119279. https://doi.org/10.1016/j.bbamcr.2022.119279.

[7] Hsu D. The dentate gyrus as a filter or gate: a look back and a look ahead. Progress in Brain Research, vol. 163, Elsevier; 2007, p. 601–13. https://doi.org/10.1016/S0079-6123(07)63032-5.

[8] Wright BJ, Jackson MB. Long-Term Potentiation in Hilar Circuitry Modulates Gating by the Dentate Gyrus. J Neurosci 2014;34:9743–53. https://doi.org/10.1523/JNEUROSCI.0814-14.2014.

[9] Bombardi C, Grandis A, Pivac N, Sagud M, Lucas G, Chagraoui A, et al. Serotonin modulation of hippocampal functions: From anatomy to neurotherapeutics. Progress in Brain Research, vol. 261, Elsevier; 2021, p. 83–158. https://doi.org/10.1016/bs.pbr.2021.01.031.

[10] Sakai N, Tanaka C. Inhibitory modulation of long-term potentiation via the 5-HT1A receptor in slices of the rat hippocampal dentate gyrus. Brain Res 1993;613:326–30. https://doi.org/10.1016/0006-8993(93)90921-9.

[11] Tecott LH, Logue SF, Wehner JM, Kauer JA. Perturbed dentate gyrus function in serotonin 5-HT $_{2C}$ receptor mutant mice. Proc Natl Acad Sci USA 1998;95:15026–31. https://doi.org/10.1073/pnas.95.25.15026.

[12] Kulla A, Manahan-Vaughan D. Modulation by Serotonin 5-HT4 Receptors of Long-term Potentiation and Depotentiation in the Dentate Gyrus of Freely Moving Rats. Cerebral Cortex 2002;12:150–62. https://doi.org/10.1093/cercor/12.2.150.

[13] Bard JA, Zgombick J, Adham N, Vaysse P, Branchek TA, Weinshank RL. Cloning of a novel human serotonin receptor (5-HT7) positively linked to adenylate cyclase. J Biol Chem 1993;268:23422–6.

[14] Lovenberg TW, Baron BM, de Lecea L, Miller JD, Prosser RA, Rea MA, et al. A novel adenylyl cyclase-activating serotonin receptor (5-HT7) implicated in the regulation of mammalian circadian rhythms. Neuron 1993;11:449–58. https://doi.org/10.1016/0896-6273(93)90149-l.

[15] Ruat M, Traiffort E, Leurs R, Tardivel-Lacombe J, Diaz J, Arrang JM, et al. Molecular cloning, characterization, and localization of a high-affinity serotonin receptor (5-HT7) activating cAMP formation. Proceedings of the National Academy of Sciences 1993;90:8547–51. https://doi.org/10.1073/pnas.90.18.8547.

[16] García-Alcocer G, Segura LCB, García Peña M, Martínez-Torres A, Miledi R. Ontogenetic distribution of 5-HT2C, 5-HT5A, and 5-HT7 receptors in the rat hippocampus. Gene Expr

2006;13:53–7. https://doi.org/10.3727/000000006783991935.
[17] Siwiec M, Kusek M, Sowa JE, Tokarski K, Hess G. 5-HT7 receptors increase the excitability of hippocampal CA1 pyramidal neurons by inhibiting the A-type potassium current. Neuropharmacology 2020;177:108248. https://doi.org/10.1016/j.neuropharm.2020.108248.
[18] Tokarski K, Zahorodna A, Bobula B, Hess G. 5-HT7 receptors increase the excitability of rat hippocampal CA1 pyramidal neurons. Brain Res 2003;993:230–4. https://doi.org/10.1016/j.brainres.2003.09.015.
[19] Gong S, Zheng C, Doughty ML, Losos K, Didkovsky N, Schambra UB, et al. A gene expression atlas of the central nervous system based on bacterial artificial chromosomes. Nature 2003;425:917–25. https://doi.org/10.1038/nature02033.
[20] Schindelin J, Arganda-Carreras I, Frise E, Kaynig V, Longair M, Pietzsch T, et al. Fiji: an open-source platform for biological-image analysis. Nat Methods 2012;9:676–82. https://doi.org/10.1038/nmeth.2019.
[21] Ting JT, Lee BR, Chong P, Soler-Llavina G, Cobbs C, Koch C, et al. Preparation of Acute Brain Slices Using an Optimized N-Methyl-D-glucamine Protective Recovery Method. J Vis Exp 2018. https://doi.org/10.3791/53825.
[22] Campagnola L, Kratz MB, Manis PB. ACQ4: an open-source software platform for data acquisition and analysis in neurophysiology research. Front Neuroinform 2014;8:3. https://doi.org/10.3389/fninf.2014.00003.
[23] Bender RA, Soleymani SV, Brewster AL, Nguyen ST, Beck H, Mathern GW, et al. Enhanced expression of a specific hyperpolarization-activated cyclic nucleotide-gated cation channel (HCN) in surviving dentate gyrus granule cells of human and experimental epileptic hippocampus. J Neurosci 2003;23:6826–36.
[24] Harden SW, Frazier CJ. Oxytocin depolarizes fast-spiking hilar interneurons and induces GABA release onto mossy cells of the rat dentate gyrus. Hippocampus 2016;26:1124–39. https://doi.org/10.1002/hipo.22595.
[25] Anderson WW, Collingridge GL. Capabilities of the WinLTP data acquisition program extending beyond basic LTP experimental functions. Journal of Neuroscience Methods 2007;162:346–56. https://doi.org/10.1016/j.jneumeth.2006.12.018.
[26] Bliss TVP, Collingridge GL, Morris RGM, Reymann KG. Long-term potentiation in the hippocampus: discovery, mechanisms and function. Neuroforum 2018;24:A103–20. https://doi.org/10.1515/nf-2017-A059.
[27] Beaudet G, Paizanis E, Zoratto F, Lacivita E, Leopoldo M, Freret T, et al. LP-211, a selective 5-HT7 receptor agonist, increases novelty-preference and promotes risk-prone behavior in rats. Synapse 2017;71. https://doi.org/10.1002/syn.21995.
[28] Comitato A, Lacivita E, Leopoldo M, Bardoni R. 5-HT7 Receptors Regulate Excitatory-Inhibitory Balance in Mouse Spinal Cord Dorsal Horn. Front Mol Neurosci 2022;15. https://doi.org/10.3389/fnmol.2022.946159.
[29] Costa L, Spatuzza M, D'Antoni S, Bonaccorso CM, Trovato C, Musumeci SA, et al. Activation of 5-HT7 serotonin receptors reverses metabotropic glutamate receptor-mediated synaptic plasticity in wild-type and Fmr1 knockout mice, a model of Fragile X syndrome. Biol Psychiatry 2012;72:924–33. https://doi.org/10.1016/j.biopsych.2012.06.008.
[30] Hedlund PB, Leopoldo M, Caccia S, Sarkisyan G, Fracasso C, Martelli G, et al. LP-211 is a brain penetrant selective agonist for the serotonin 5-HT7 receptor. Neurosci Lett 2010;481:12–6. https://doi.org/10.1016/j.neulet.2010.06.036.
[31] Lippiello P, Hoxha E, Speranza L, Volpicelli F, Ferraro A, Leopoldo M, et al. The 5-HT7 receptor triggers cerebellar long-term synaptic depression via PKC-MAPK. Neuropharmacology 2016;101:426–38. https://doi.org/10.1016/j.neuropharm.2015.10.019.

[32] Pernía-Andrade AJ, Goswami SP, Stickler Y, Fröbe U, Schlögl A, Jonas P. A deconvolution-based method with high sensitivity and temporal resolution for detection of spontaneous synaptic currents in vitro and in vivo. Biophys J 2012;103:1429–39. https://doi.org/10.1016/j.bpj.2012.08.039.
[33] Winchester G, Liu S, Steele OG, Aziz W, Penn A. Eventer. Software for the detection of spontaneous synaptic events measured by electrophysiology or imaging 2020. https://doi.org/10.5281/zenodo.3991677.
[34] Posit team. RStudio: Integrated Development Environment for R 2024.
[35] R Core Team. R: A Language and Environment for Statistical Computing 2024.
[36] Wickham H, Averick M, Bryan J, Chang W, McGowan LD, François R, et al. Welcome to the tidyverse. Journal of Open Source Software 2019;4:1686. https://doi.org/10.21105/joss.01686.
[37] Pedersen TL. patchwork: The Composer of Plots 2024.
[38] Amaral DG, Scharfman HE, Lavenex P. The dentate gyrus: fundamental neuroanatomical organization (dentate gyrus for dummies). In: Scharfman HE, editor. Progress in Brain Research, vol. 163, Elsevier; 2007, p. 3–790. https://doi.org/10.1016/S0079-6123(07)63001-5.
[39] Sun Y, Grieco SF, Holmes TC, Xu X. Local and Long-Range Circuit Connections to Hilar Mossy Cells in the Dentate Gyrus. eNeuro 2017;4. https://doi.org/10.1523/ENEURO.0097-17.2017.
[40] Scharfman HE. The enigmatic mossy cell of the dentate gyrus. Nat Rev Neurosci 2016;17:562–75. https://doi.org/10.1038/nrn.2016.87.
[41] Scharfman HE. Electrophysiological evidence that dentate hilar mossy cells are excitatory and innervate both granule cells and interneurons. J Neurophysiol 1995;74:179–94. https://doi.org/10.1152/jn.1995.74.1.179.
[42] Botterill JJ, Lu Y-L, LaFrancois JJ, Bernstein HL, Alcantara-Gonzalez D, Jain S, et al. An Excitatory and Epileptogenic Effect of Dentate Gyrus Mossy Cells in a Mouse Model of Epilepsy. Cell Rep 2019;29:2875-2889.e6. https://doi.org/10.1016/j.celrep.2019.10.100.
[43] Santhakumar V, Bender R, Frotscher M, Ross ST, Hollrigel GS, Toth Z, et al. Granule cell hyperexcitability in the early post-traumatic rat dentate gyrus: the 'irritable mossy cell' hypothesis. The Journal of Physiology 2000;524:117–34. https://doi.org/10.1111/j.1469-7793.2000.00117.x.
[44] Ma Y, Bayguinov PO, McMahon SM, Scharfman HE, Jackson MB. Direct synaptic excitation between hilar mossy cells revealed with a targeted voltage sensor. Hippocampus 2021;31:1215–32. https://doi.org/10.1002/hipo.23386.
[45] Espinoza C, Guzman SJ, Zhang X, Jonas P. Parvalbumin+ interneurons obey unique connectivity rules and establish a powerful lateral-inhibition microcircuit in dentate gyrus. Nat Commun 2018;9:4605. https://doi.org/10.1038/s41467-018-06899-3.
[46] Hosp JA, Strüber M, Yanagawa Y, Obata K, Vida I, Jonas P, et al. Morpho-physiological criteria divide dentate gyrus interneurons into classes. Hippocampus 2014;24:189–203. https://doi.org/10.1002/hipo.22214.
[47] Savanthrapadian S, Meyer T, Elgueta C, Booker SA, Vida I, Bartos M. Synaptic properties of SOM- and CCK-expressing cells in dentate gyrus interneuron networks. J Neurosci 2014;34:8197–209. https://doi.org/10.1523/JNEUROSCI.5433-13.2014.
[48] Yuan M, Meyer T, Benkowitz C, Savanthrapadian S, Ansel-Bollepalli L, Foggetti A, et al. Somatostatin-positive interneurons in the dentate gyrus of mice provide local- and long-range septal synaptic inhibition. Elife 2017;6. https://doi.org/10.7554/eLife.21105.
[49] Kusek M, Siwiec M, Sowa JE, Bobula B, Bilecki W, Ciurej I, et al. 5-HT7 receptors enhance inhibitory synaptic input to principal neurons in the mouse basal amygdala. Neuropharmacology 2021;198:108779. https://doi.org/10.1016/j.neuropharm.2021.108779.

[50] Tokarski K, Kusek M, Hess G. 5-HT7 receptors modulate GABAergic transmission in rat hippocampal CA1 area. J Physiol Pharmacol 2011;62:535–40.
[51] Amaral DG. A golgi study of cell types in the hilar region of the hippocampus in the rat. Journal of Comparative Neurology 1978;182:851–914. https://doi.org/10.1002/cne.901820508.
[52] Larson J, Munkácsy E. Theta-burst LTP. Brain Res 2015;1621:38–50. https://doi.org/10.1016/j.brainres.2014.10.034.
[53] Spyrka J, Hess G. Repeated restraint-induced modulation of long-term potentiation in the dentate gyrus of the mouse. Brain Res 2010;1320:28–33. https://doi.org/10.1016/j.brainres.2010.01.031.
[54] Djavadian RL. Serotonin and neurogenesis in the hippocampal dentate gyrus of adult mammals. Acta Neurobiol Exp 2004;64:189–200.
[55] Le Corre S, Sharp T, Young AH, Harrison PJ. Increase of 5-HT7 (serotonin-7) and 5-HT1A (serotonin-1A) receptor mRNA expression in rat hippocampus after adrenalectomy. Psychopharmacology 1997;130:368–74. https://doi.org/10.1007/s002130050252.
[56] Medrihan L, Sagi Y, Inde Z, Krupa O, Daniels C, Peyrache A, et al. Initiation of Behavioral Response to Antidepressants by Cholecystokinin Neurons of the Dentate Gyrus. Neuron 2017;95:564-576.e4. https://doi.org/10.1016/j.neuron.2017.06.044.
[57] Brandon NJ, McKay R. The cellular target of antidepressants. Nat Neurosci 2015;18:1537–8. https://doi.org/10.1038/nn.4144.
[58] Nozaki K, Kubo R, Furukawa Y. Serotonin modulates the excitatory synaptic transmission in the dentate granule cells. J Neurophysiol 2016;115:2997–3007. https://doi.org/10.1152/jn.00064.2016.
[59] Núñez-Ochoa MA, Chiprés-Tinajero GA, Medina-Ceja L. Evaluation of the hippocampal immunoreactivity of the serotonin 5-HT1A, 5-HT2 and 5-HT7 receptors in a pilocarpine temporal lobe epilepsy rat model with fast ripples. Neuroreport 2021;32:306–11. https://doi.org/10.1097/WNR.0000000000001594.
[60] Sagi Y, Medrihan L, George K, Barney M, McCabe KA, Greengard P. Emergence of 5-HT5A signaling in parvalbumin neurons mediates delayed antidepressant action. Mol Psychiatry 2020;25:1191–201. https://doi.org/10.1038/s41380-019-0379-3.
[61] Palacios JM. Serotonin receptors in brain revisited. Brain Res 2016;1645:46–9. https://doi.org/10.1016/j.brainres.2015.12.042.
[62] Kawa K. Distribution and functional properties of 5-HT3 receptors in the rat hippocampal dentate gyrus: a patch-clamp study. Journal of Neurophysiology 1994;71:1935–47. https://doi.org/10.1152/jn.1994.71.5.1935.